IOPscience iopscience.iop.org

Home Search Collections Journals About Contact us My IOPscience

d-to-s bonding in GaN

This article has been downloaded from IOPscience. Please scroll down to see the full text article.

1998 J. Phys.: Condens. Matter 10 7155

(http://iopscience.iop.org/0953-8984/10/32/007)

View the table of contents for this issue, or go to the journal homepage for more

Download details:
IP Address: 171.66.16.209
The article was downloaded on 14/05/2010 at 16:40

Please note that terms and conditions apply.

J. Phys.: Condens. Matter **10** (1998) 7155–7162. Printed in the UK PII: S0953-8984(98)92831-4

d-to-s bonding in GaN

P Dudešek†‖, Ľ Benco†¶, C Daul‡ and K Schwarz§

† Institute of Inorganic Chemistry, Slovak Academy of Sciences, Dúbravská cesta 9, SK-84236 Bratislava, Slovak Republic

‡ Institute of Inorganic Chemistry, University of Fribourg, Perolles, CH-1700 Fribourg, Switzerland

§ Vienna University of Technology, Getreidemarkt 9/158, A-1060 Vienna, Austria

Received 30 March 1998, in final form 20 May 1998

Abstract. The interaction scheme for cubic GaN is constructed from the FP-LAPW density of states and scalar relativistic free-atom LDA eigenvalues. Orbital interactions responsible for the DOS distribution, indicated by interaction lines, show that, due to the Ga d-to-N s bonding the d states split into three subbands, displaying ds bonding, nonbonding, and antibonding properties. While nonbonding bands comprise d states of both t_{2g} and e_g symmetry components, bonding and antibonding ds states originate exclusively from the t_{2g}-to-s orbital interactions. Due to the slight N p admixture, the relatively narrow band of nonbonding d states shows reversed tetrahedral t_{2g}–e_g splitting similar to that of fully occupied d states in II–VI semiconductors.

The physical properties of gallium nitride make this compound a candidate for use in applications in electronic devices, such as short-wavelength emitters [1–3]. An increasing technological interest has also been stimulating numerous theoretical studies, reporting band-structures [4–9], optical properties [6, 7], and phase transformations under pressure [4–6, 10, 11]. At zero pressure, the stable low-temperature modification has the W (wurtzite) structure [4–6, 10, 11]. Yeh *et al* [12, 13] have shown that the W polytype is favoured over the ZB (zinc-blende) phase due to the small atomic size of the anion. Unlike the typical III–V compound GaAs, in which practically inert Ga d states appear well below the s-like valence band, GaN represents a special case where a resonance of Ga d and N s states occurs [7, 8]. The proper treatment of the Ga d states is therefore important for understanding the properties of GaN [8]. When in the pseudopotential framework the Ga d states are treated as inert core states, a too small lattice constant is obtained [9] and the ZB structure is lower in energy than the W structure, contrary to experimental findings [1–3]. Performing all-electron calculations for the ZB phase, Fiorentini *et al* [8] have thoroughly analysed the role of the d electrons. They show the influence of d orbitals on the band-structure, cohesive properties, and charge density of GaN. In order to plot $\boldsymbol{k}$-integrated band contributions to the density, Fiorentini *et al* subdivide the valence sphere into the bottom, d, and top valence bands, as delineated by band-gaps [8]. Such classification, however, is arbitrary, because valence bands usually consist of states with different bonding properties, and partial charge densities plotted for such a group of states are rather inconclusive.

‖ Present address: Institute of Theoretical Physics, University of Graz, Universitätsplatz 5, A-8010, Graz, Austria.
¶ Present address: Institute of Inorganic Chemistry, University of Fribourg, Perolles, CH-1700 Fribourg, Switzerland.

0953-8984/98/327155+08$19.50 © 1998 IOP Publishing Ltd

In this paper we extend previous studies [4–13] with the interaction scheme of GaN. Of particular interest is the interaction between the semicore Ga 3d states and the N s states. This interaction splits pertinent levels into a multiplet, all of the states of which are occupied. No gain in energy is therefore expected to affect the cohesive properties. The scheme, however, provides insight into orbital interactions and also the classification of states according to their bonding character, which may be important in evaluating those properties of the material that depend on the covalency/ionicity of the energy states. States originating from the d-to-s interaction are displayed via both partial charge densities and partial densities of states.

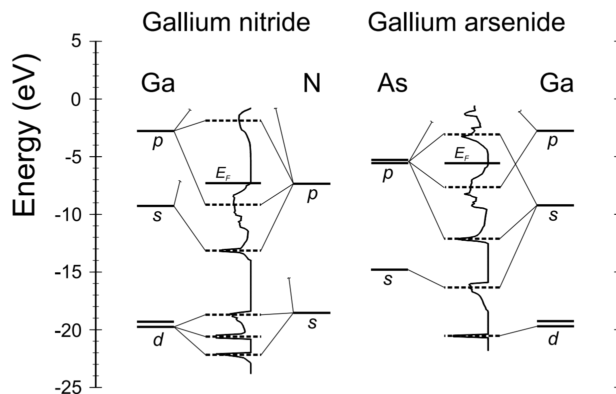

Figure 1. The interaction scheme of GaN (left). The scheme of GaAs (right) is given for reference.

Figure 1 shows the interaction schemes constructed for the ZB structures of GaN and GaAs (the latter is given for reference). It is found that an inspection of the atomic orbital energies is useful in the investigation of the interatomic interactions responsible for the DOS distribution [8, 14]. The interaction scheme represents a diagram displaying the positions of both the free-atom and the solid-state levels (DOS) on the real-energy scale. Interaction lines, indicating the splitting of the atomic states according to their role in the bonding, then make the scheme self-explanatory (the procedure for the construction of a scheme is described in [15, 16]; the scheme for GaN can be found in [17]). In figure 1, all-electron FP-LAPW electronic structures (within experimental geometries: $a = 4.531$ Å (GaN) and 5.653 Å (GaAs)) and scalar relativistic free-atom LDA eigenvalues are used [18]. The exchange and correlation potential is parametrized following Perdew and Wang [19]. Angular momenta up to $l_{max} = 10$ in the muffin-tin spheres (with radii $R = 2.15$ au and 1.55 au for Ga and N, respectively) and plane waves with wave vectors up to $k_{\rm max} = 5.16$ au are used, as is the Monkhorst–Pack [20] 30-special-point mesh. The spin–orbit (SO) coupling is added as a formal perturbation to the Hamiltonian as implemented in the WIEN97 code [21] according to MacDonald *et al* [22]. Figure 2 shows the angular-momentum-projected DOS of GaN which are used to assign interaction lines. In figure 1 these lines are sketched for major bunches of partial DOS. Small contributions are omitted for clarity. Note that the energy scales in figures 1 and 2 are different. In figure 2 the scale is relative to the valence-band maximum. In figure 1, however, the total DOS of GaN and GaAs are shifted to fix the band of the d nonbonding states at the value of the experimental binding energy of Ga 3d orbitals ($E_B \approx -20.5$ eV [23]). For GaN the position of the sharp peak of practically pure d states (in figure 2 situated at ≈ -13.5 eV) is taken *a priori* as a band

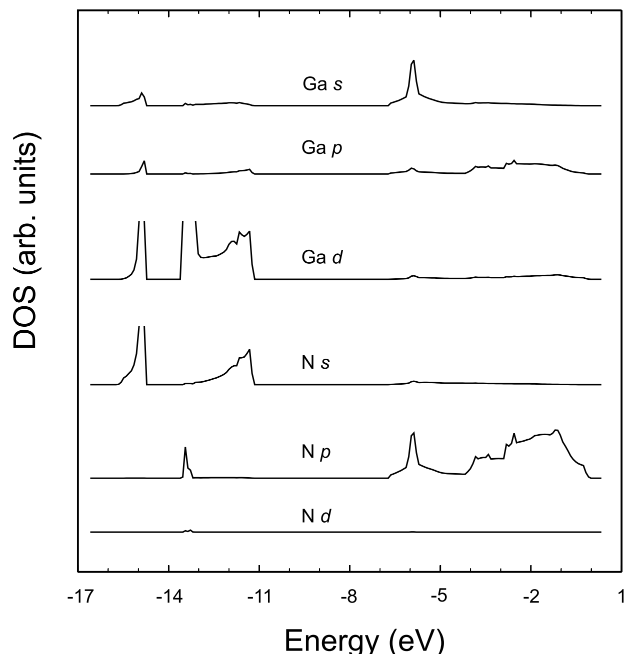

Figure 2. The angular momentum decomposition of the atom-projected densities of states. From top to bottom: Ga s, p, and d states, and N s, p, and d states (zeroed to the position of the Fermi level).

of the d nonbonding states.

The schemes in figure 1 are in fact solid-state analogues of the widely used molecular orbital schemes. They show in simple terms many characteristic features of the bonding, such as orbital interactions, bonding properties of states, and covalency/ionicity relations [15–17]. The schemes show the 2:2 pattern of the bonding in GaAs. For GaN, in contrast, the 3:2 pattern occurs (three levels of Ga interact with two levels of N). The new feature in GaN is the d-to-s bonding at the bottom of the valence region. This interaction causes the dispersion of the ds states over an energy interval of $\approx$5 eV. They are gathered in three bands, the lowest two of them separated by a gap (cf. figures 1, 2 and figures in references [7] and [8]).

An effective bonding is driven by two factors: the overlap between atomic orbitals and the energy matching of interacting levels (ΔE_{ab} for orbitals a and b). When $\Delta E \approx 0$ the interaction is covalent. In such a case the powers of the pertinent atomic levels to attract electrons to themselves are similar. An interaction of this kind causes an increase of the electron density in the interatomic region which contains mixed orbitals centred at both interacting atoms. The corresponding covalent states are easily recognized according to the mirroring of the orbital-projected DOS on the energy scale (figure 2). The advantage of the interaction scheme (figure 1) is the displaying of the true free-atom energy levels, the mutual positioning of which indicates the degree of covalency without displaying the partial DOS. As for the d-to-s interaction, the scheme shows a relatively small value of $\Delta E_{\rm ds}$. Using free-atom LDA eigenvalues, this value for the two SO components of the d level amounts to 0.73 and 1.20 eV, respectively. The d-to-s interaction within the LDA leads to a dispersion of states of $\approx$5 eV. This is smaller than the experimental value, which is $\approx$6 eV [24]. A

better dispersion is obtained when the self-interaction correction (SIC) is taken into account [25]. The SIC brings the free-atom eigenvalues for the Ga 3d and N 2s levels closer together ($\Delta E_{ds} = 0.31$ and 0.78 eV), and this improved energy matching produces more covalent bonding and a larger dispersion of the ds states. Recently, Rohlfing *et al* [26] have shown that the GW approximation gives improved dispersion, as well as a more realistic shape for the DOS. In their band-structure, the two lowest bands are overlapped, which is in good agreement with the photoelectron spectrum of GaN [24]. In spite of the known drawback of the LDA of the dispersion of the ds states and the separation of the three subbands, our analysis is performed within the LDA. In fact, we take advantage of the band separation in analysing the bonding properties of the semicore states and to enhance our understanding of the bonding mechanism. In figure 1 the covalency of states resulting from the mixing of the orbitals of two neighbouring atoms is indicated by a pair of interaction lines. Two lines for each bunch of covalent states indicate the orbital interaction responsible for the creation of the pertinent states.

For both compounds, two bands just below E_F are due to the M(p)-to-X(p) and M(s)-to-X(p) orbital interactions (M and X denote the metal and the nonmetal atom, respectively), and show similar dispersion. For GaN, however, both bands are shifted downwards due to the deeper-lying N p level, compared to that of As (cf. the electronegativities of these two atoms). For the inner valence region, the interaction schemes show pronounced differences. In GaAs the As s level 'prefers' the s-to-s interaction ($\Delta E_{ss} \cong 5.6$ eV) to the s-to-d interaction ($\Delta E_{sd} \cong 4.7$ eV), probably because of the much larger overlap between s orbitals in the tetrahedral arrangement as compared to that with contracted inner d orbitals. The d orbitals in GaAs thus remain inert. In GaN, the improved energy matching ($\Delta E_{ds}^{LDA} = 0.73$ and 1.20 eV, respectively) enables efficient d-to-s bonding to occur. Interaction lines (cf. figure 1) indicate that the multiplet of d states is classified into three subbands according to their bonding properties. The bottom valence band at (≈ -22 eV) consists of bonding ds states. The bonding character of these states is indicated by the directions of the interaction lines. When coming down from the atomic positions to the position in the solid, they indicate a stabilizing shift due to the bonding. For the subband of d states centred at -20.5 eV there is only one interaction line. These states are nonbonding. Having no counterpart for the covalent bonding, they reside on the Ga atom. The interaction line shows that in a solid the nonbonding d states are slightly stabilized compared to those of free atoms (cf. the position of this band in the schemes for GaN and GaAs). For the rest of the d states spread by up to ≈ -18.5 eV, the interaction line indicates an antibonding character, because they are destabilized as compared to d levels of free Ga atoms.

Figure 3 shows partial $\boldsymbol{k}$-integrated charge densities of d states in GaN plotted in a (110) plane containing two Ga atoms (lower corners) and one N atom (centre). The contour-line spacing of the charge-density plots is 0.05 electrons Å^{-3} (cut off at the value of 0.5 electrons Å^{-3}). The densities are displayed for states within energy windows classified according to the interaction scheme (see above) into three categories.

(i) The charge density for the ds bonding states displayed in figure 3(c) is identical to that of the bottom valence band presented in figure 7 of reference [12]. It is increased along the bond direction as expected for the covalent interaction.

(ii) Pure d states concentrated in the sharp narrow band (centred at -20.5 eV) are classified as nonbonding. Figure 3(b) shows that the charge densities plotted for these states reside exclusively on the Ga atoms.

(iii) Finally, figure 3(a) displays the charge density for the ds antibonding states. Originating from two neighbouring atoms, this density keeps away from the bond centre.

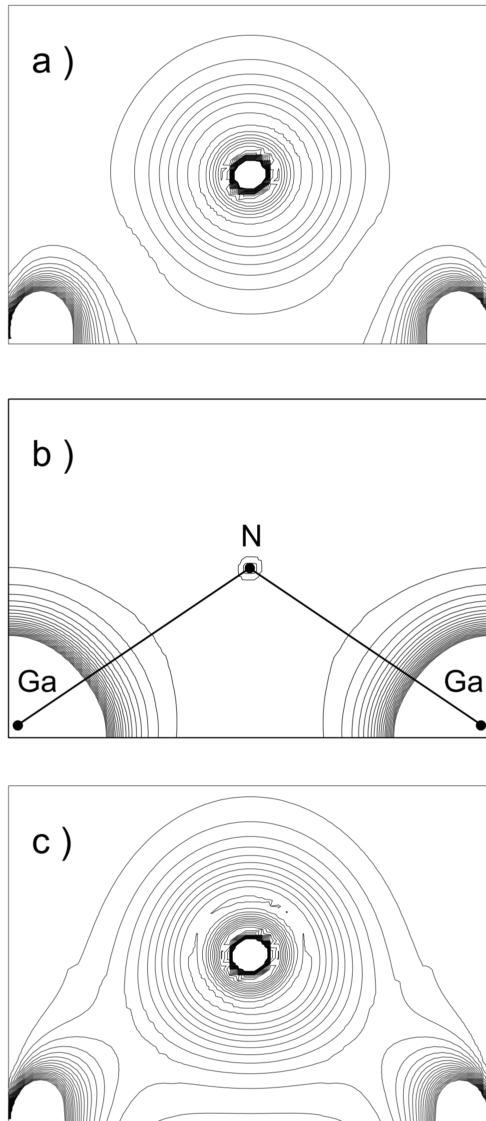

Figure 3. Partial $\boldsymbol{k}$-integrated charge densities in GaN for the antibonding ds states (a), the nonbonding d states (b), and the bonding ds states (c).

In spite of the imperfect separation of the d nonbonding and ds antibonding states (the integrated electron densities are 8.157 and 1.842 instead of 8 and 2 electrons), figure 3, based on the classification in the interaction scheme, provides additional insight into the bonding mechanism of GaN.

Figure 4 displays in detail the states involved in the d-to-s interaction, the d states being decomposed into t_{2g} and e_g symmetry components. As shown in figure 4(a), both the ds bonding (≈ -22 eV) and the ds antibonding (spread by up to ≈ -18.5 eV) states consist of N s and Ga t_{2g} components. In the tetrahedral environment only the t_{2g} orbitals of the central atom can reach the orbitals of the four N atoms at the corners of a tetrahedron.

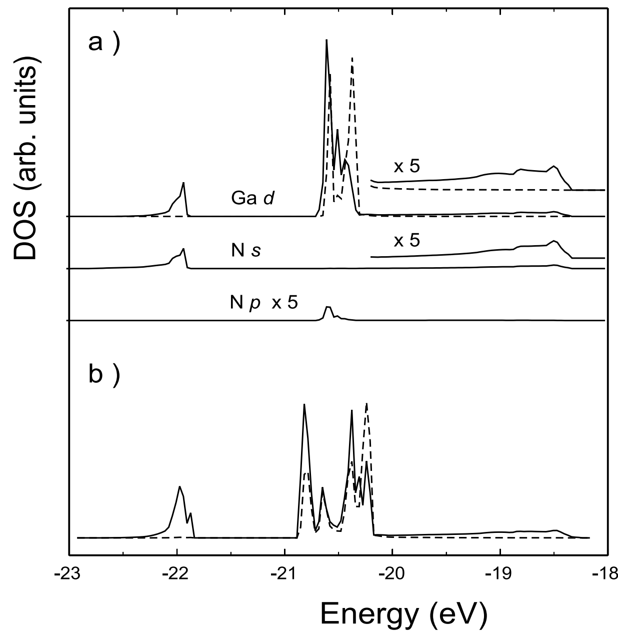

Figure 4. (a) Detail of the d bands of GaN without the spin–orbit coupling. From top to bottom: Ga d t_{2g} (——) and e_g (- - - -) symmetry components, N s, and p partial DOS. (b) The d bands after switching on the spin–orbit coupling. The energy scale is as in figure 1.

Figure 4(a) demonstrates that the efficient d-to-s bonding originates from orbital interactions of the t_{2g} orbitals with the surrounding N s orbitals. Note that the relatively narrow band of the nonbonding d states shows a slight splitting ($\approx$0.4 eV) into t_{2g} and e_g components with the reversed tetrahedral ordering. The concept of the splitting of a set of degenerate d energy levels in a symmetrical environment was developed for *partly filled* d orbitals. A tetrahedral field due to the charge density around the metal atom separates the d orbitals into two symmetry components. The t_{2g} orbitals contact orbitals of neighbouring atoms. Due to the repulsion of negative charge densities, these levels are raised in energy. In contrast, the e_g orbitals point between the corners of a tetrahedron. The accommodation of the d charge density in these orbitals therefore minimizes the repulsion and makes them energetically favoured (see textbook discussions in, e.g., [27, 28]). This mechanism, however, cannot apply when d levels are *fully occupied*. The role of d states in the bonding of II–VI semiconductors, having the d band below the valence p band in the heteropolar gap, was extensively investigated by Wei and Zunger [14]. On the basis of an analysis of the energy levels and wavefunctions within the high-symmetry points of the Brillouin zone, which are not representative of the bonding in a solid, they observed that the altered sign of the crystal-field splitting is due to the p–d repulsion. A similar conclusion was formulated for GaN using similar arguments [8]. The partial DOS displayed in figure 4(a) show that the reversed crystal-field splitting is valid not only for the high-symmetry points, but also for $\boldsymbol{k}$-integrated quantities. Figure 4(a) shows that in GaN the nonbonding d states are separated into two components due to orbital interactions of the t_{2g} orbitals with the N p electron density. For this interaction, the large value of $\Delta E_{pd} = 12.2$ eV (figure 1) prevents effective p-to-d bonding. The symmetry-allowed overlap, however, causes slight M(d)-to-X(p) mixing which stabilizes the t_{2g} components of the multiplet of the d nonbonding states.

The SO coupling of atomic Ga 3d levels is ≈0.5 eV. In figure 1 this splitting is indicated by doubled horizontal lines. The value of the SO splitting is comparable to the crystal-field splitting of the nonbonding d states displayed in figure 4(a). The combined effect of the SO and the crystal-field splitting is shown in figure 4(b). Comparison of figures 4(a) and 4(b) shows that the SO coupling has a negligible influence on the ds bonding and the ds antibonding states. The nonbonding states, centred at ≈−20.5 eV, are spread over an energy interval approximately twice as large as that in the case without SO coupling. The band now has four components. The partial DOS projected into t_{2g} and e_g symmetries again shows the dominant t_{2g} character of the lowest bands and the pronounced e_g character of the topmost nonbonding states.

In summary, the interaction scheme of GaN shows splitting of the semicore Ga 3d states due to the d-to-s interaction into three groups of bands according to their bonding properties. Only t_{2g} orbitals overlapping orbitals of the surrounding nitrogen atoms participate in bonding (antibonding) interactions. The nonbonding states of the main d band arise due to the slight admixture of N p states separated into t_{2g} and e_g components showing reversed tetrahedral ordering. The SO coupling doubles the nonbonding d bands but preserves the ordering of the symmetry components.

Acknowledgments

The support of the Slovak Grant Agency VEGA is acknowledged (Grant No 1172). The authors thank C Ambrosch-Draxl for help with the SO treatment. The manuscript was greatly improved as a result of constructive criticism from an anonymous referee.

References

[1] Martin G, Strite S, Thornton J and Morkoc H 1991 *Appl. Phys. Lett.* **58** 2375
[2] Strite A and Morkoc H 1992 *J. Vac. Sci. Technol.* B **10** 1237
[3] Davis R F 1991 *Proc. IEEE* **79** 702
[4] Gorczyca I and Christensen N E 1991 *Solid State Commun.* **80** 335
[5] Perlin P, Gorczyca I, Christensen N E, Grzegory I, Teisseyre H and Suski T 1992 *Phys. Rev.* B **45** 13 307
[6] Christensen N E and Gorczyca I 1994 *Phys. Rev.* B **50** 4397
[7] Xu Y N and Ching W Y 1993 *Phys. Rev.* B **48** 4335
[8] Fiorentini V, Methfessel M and Scheffler M 1993 *Phys. Rev.* B **47** 13 353
[9] Min B J, Chan C T and Ho K M 1992 *Phys. Rev.* B **45** 1159
[10] Munoz A and Kunc K 1991 *Phys. Rev.* B **44** 10 372
[11] Pandey R, Causà M, Harrison N M and Seel M 1996 *J. Phys.: Condens. Matter* **8** 3993
[12] Yeh C Y, Lu Z W, Froyen S and Zunger A 1992 *Phys. Rev.* B **45** 12 130
[13] Yeh C Y, Lu Z W, Froyen S and Zunger A 1992 *Phys. Rev.* B **46** 10 086
[14] Wei S-H and Zunger A 1988 *Phys. Rev.* B **37** 8958
[15] Benco Ľ 1995 *Solid State Commun.* **94** 861
[16] Benco Ľ 1998 *Ceram. Int.* at press
[17] Benco Ľ 1996 Ψ_k *Network Conf.* (Schwäbisch Gmünd: Max-Planck-Institut für Festkörperforschung) programme and abstracts, p 102
[18] Blaha P, Schwarz K, Dufek P and Augustyn R 1995 *Wien95: User's Guide* (Vienna: Technical University Vienna)
[19] Perdew J P and Wang Y 1992 *Phys. Rev.* B **45** 13 244
[20] Monkhorst H J and Pack D J 1976 *Phys. Rev.* B **13** 5188
[21] Novák P, Harmon B F, Persson C, Blaha P, Diviš M, Eschrig H and Richter M 1998 to be published
[22] MacDonald A H, Pickett W E and Koelling D D 1980 *J. Phys. C: Solid State Phys.* **13** 2675
[23] Carlson T A 1975 *Photoelectron and Auger Spectroscopy* (New York: Plenum)
[24] Ding S A, Neuhold G, Weaver J H, Häberle P, Horn K, Brandt O, Yang H and Ploog K 1996 *J. Vac. Sci. Technol.* A **14** 819

[25] Perdew J P, Chevary J A, Vosko S H, Jackson K A, Pederson M R, Singh D J and Fiolhais C 1992 *Phys. Rev.* B **46** 6671
[26] Rohlfing M, Krüger P and Pollman J 1998 *Phys. Rev.* B **57** 6485
[27] Figgis B 1966 *Introduction to Ligand Field Theory* (New York: Interscience)
[28] Huheey J E 1978 *Inorganic Chemistry* (New York: Harper and Row)